Experimental Details

Materials: Nickel nitrate ($Ni(NO_3)_2 \cdot 6H_2O$, 99.9%, Strem Chemicals), cobalt nitrate ($Co(NO_3)_2 \cdot 6H_2O$, 99+% of analytical grade, Acros Organics) and iron nitrate ($Fe(NO_3)_3 \cdot 9H_2O$, ≥98%, Sigma-Aldrich) as well as sodium nitrate ($NaNO_3$, ≥99%, Acros Oragnics) were used as received for the synthesis. Formamide (99.5+%) was purchased from Acros Organics and sodium hydroxide (99.99%) was obtained from Sigma-Aldrich. All deionized water used in this work was generated from Milli-Q® Ultrapure Water System (Millipore, Bedford, USA). For the isotope labelling experiment, ^{18}O-water (97 atom % ^{18}O) was purchased from Sigma-Aldrich.

Synthesis of Ni, NiCo and NiFe LDH nanosheets: A previously reported method was modified to directly synthesize Ni, NiCo and NiFe LDH nanosheets using a layer growth inhibitor, formamide.[1] For fabrication of the Ni LDH nanosheets, a 10.0 mL solution containing 50 mM $(Ni(NO_3)_2 \cdot 6H_2O$ was dropwise added to a 20.0 mL solution of 10 mM $NaNO_3$ containing 23 vol% formamide as an inhibitor. The solution was heated at 80 °C with stirring and 0.25 M NaOH that was purified to remove Fe impurities, was added drop by drop to maintain the solution pH at about 10. NiCo and NiFe LDH nanosheets were fabricated in a similar way. For the synthesis of NiCo nanosheets, the solution containing 37.5 mM $(Ni(NO_3)_2 \cdot 6H_2O$ and 12.5 mM $Co(NO_3)_2 \cdot 6H_2O$ was used and for the NiFe synthesis the solution containing 37.5 mM $(Ni(NO_3)_2 \cdot 6H_2O$ and 12.5 mM $Fe(NO_3)_2 \cdot 9H_2O$ was used. For NiCoFe, the precursor solution was composed of 37.5 mM $(Ni(NO_3)_2 \cdot 6H_2O$, 10.0 mM $Co(NO_3)_2 \cdot 6H_2O$ and 2.5 mM $Fe(NO_3)_2 \cdot 9H_2O$. The reaction was completed within 10 min. After that, the samples were cooled at room temperature and centrifuged and washed with ethanol and deionized water (1:1 by vol%). The washing process was repeated for at least 3 times. The LDH nanosheets were dispersed in degassed formamide and kept in the wet state for subsequent electrochemical test and in-situ Raman analysis.

Sample characterizations: Atomic compositions of the synthesized samples were determined by ICP-OES (5110 ICP-OES, Agilent Technologies). For the measurement, each catalyst was added dropwise to 10 vol% ultrapure nitric acid (65%, Merck KGaA) and then analyzed with RSD within 2%. For TEM images, a catalyst ink was added to ethanol and diluted and then deposited dropwise onto carbon coated copper grids. All the TEM measurements were

performed by FEI Titan Themis 60-300 kV. For AFM sample preparation, a catalyst ink was diluted with ethanol and a few drops of the diluted ink were dispersed on a highly oriented pyrolytic graphite (HOPG, Alfa Aesar) that was oxidized by oxygen-plasma treatment (Femto, Diener Electronic). The catalyst-loaded HOPG was rotated on a spin-coater (WS-650-23B, Laurell Technologies) at 1000 rpm and 3000 rpm successively for 30 sec and 300 sec. Finally, the sample was washed with deionized water and then dried at 125°C. AFM measurements were performed using a Dimension FastScan AFM (Bruker) with NanoScope version 8.15 software and a NanoScope V Controller (Bruker) operating in PeakForce Quantitative Nano-Mechanics (PF-QNM) mode. The FastScan-C probes (Bruker) with a spring constant of 0.8 N/nm and tip radius of 5 nm were used. Ex-situ measurements of NiFe LDH sheets were performed in air, while AFM experiments of NiCo and Ni LDH nanosheets were performed in 0.1 M KOH to have a realistic measurement of the nanosheets height profiles at the solid/liquid interface. For the experiments, 0.1 M KOH (80 μL) was deposited directly on the AFM head with the mounted cantilever. Careful approach enables the formation of a capillary bridge between the hanging droplet on the AFM head and the sample. For typical imaging conditions, AFM images were collected at scan frequencies of 1 to 5 Hz, while applying loading up to 150 pN. All images were analyzed using the WSxM 5.0 software.[2]

Electrochemical test conditions: The electrochemical measurements were carried out on a multichannel potentiostat / galvanostat (VSP, Bio-Logic) using a three-electrode system in a custom made electrochemical cell (see Figure S2) constructed by a mechanical workshop. All the measurements were performed in Fe-free KOH solutions. The Fe-free KOH solutions were prepared according to a procedure reported by the Boettcher group.[3] A double junction Ag/AgCl electrode with saturated KCl filling solution was used as a reference electrode and a Pt wire was used as a counter electrode. The linear sweep voltammetry curves were obtained at a scan rate of 1 mV sec^{-1} and IR drop was compensated at a rate 90% by default through Bio-Logic EC-Lab software. All the electrochemical measurements in this work were exhibited in reversible hydrogen electrode (RHE) scale by following equation:

$$E\ (V\ vs.\ RHE) = E\ (V\ vs.\ Ag/AgCl) + 0.197\ V + 0.0592 \times pH$$

Electrode preparation: The synthesized colloids mixed with formamide with a ratio of 0.5 mg :1 mL were directly used. First, the colloid was sonicated for at least 10 min to make it dispersed

homogeneously. 20 μL of the colloid containing nanosheet catalyst was then drop-casted on a gold substrate that was roughened *via* an electrochemical treatment for *in-situ* Raman spectroscpoy experiments. Afterwards, the catalyst-loaded gold was dried at 125°C to evaporate the solvent.

In-situ Raman spectroscopy: All the *in-situ* Raman spectroscopy experiments were carried out at a Raman spectroscopy (inVia confocal Raman microscope, Renishaw) with a 63× water immersion objective (Leica-Microsystems). The objective was wrapped in a Teflon film (0.001 in thickness, McMaster Carr) to prevent direct contact between the lens and electrolyte. Laser excitation was conducted at 532 nm with a laser power of ~0.3 mW at a grating of 1800 l mm^{-1}. The estimated diameter of the laser spot was ~0.72 μm calculated from following equation:

Diameter of laser spot = (1.22 × λ) / NA

Where λ is the wavelength of the laser, and NA is the numerical aperture of the working objective. Experiments to investigate lattice oxygen exchange of the as-synthesized samples in the absence of applied potentials were performed at 785 nm with a laser power of ~0.35 mW at a grating of 1200 l mm^{-1} to obtain the surface enhanced Raman scattering (SERS) effect. The scattered light was collected by the water immersion objective and then directed to charge coupled device (CCD) detector. Prior to use, the Raman shift range was calibrated using the 520 ± 0.5 cm^{-1} peak of silicon. Each *in-situ* spectrum was recorded with a resolution of ~1 cm^{-1} by accumulating 20 scans. The exposure time was 3 sec for each spectrum. The working electrode used in this work was a gold foil back-contacted with a copper wire. Prior to each experiment, the gold foil was mechanically polished using a commercially available polishing pad with alumina powder (0.3 μm) and then immersed in a mixture of ethanol and acetone at volumetric ratio of 1:1 for subsequent sonication. The sonication was performed at least for 10 min and repeated several times. The polished gold surface was electrochemically roughened by 20 oxidation-reduction cycles between -0.3 V and 1.3 V *vs.* Ag/AgCl in 0.1 M KCl solution. During the electrochemical treatment, the potential was held for 30 sec at the negative limit and 1.3 sec at the positive limit. The roughening procedure is well known for the effect as surface-enhanced resonance Raman scattering.[4] The roughened gold surface was thoroughly rinsed with water. Finally, catalyst colloid was drop-casted on the roughened gold electrode and then assembled to the custom-made electrochemical cell.

Table S1. Atomic ratio determined by ICP-OES

	Samples			
Elements	Ni	NiCo	NiFe	NiCoFe
Ni	99.955	75.394	75.104	74.956
Co	-	24.606	-	20.161
Fe	0.045	-	24.896	4.883

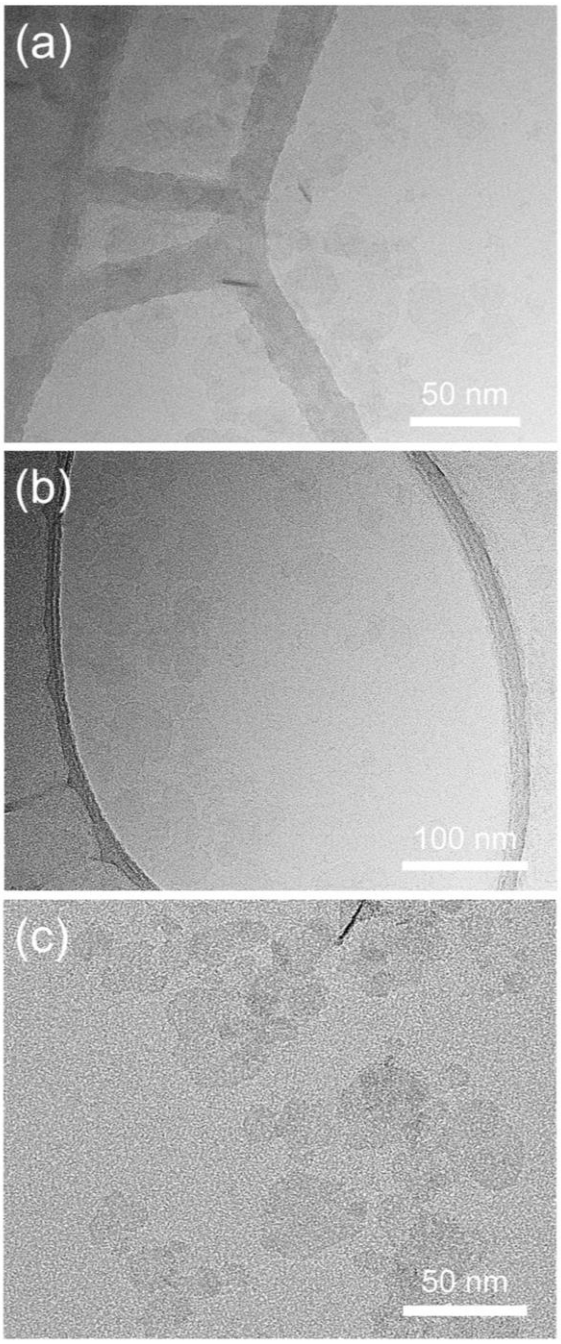

Figure S1. TEM images of (a) Ni, (b) NiCo and (c) NiFe LDH nanosheets.

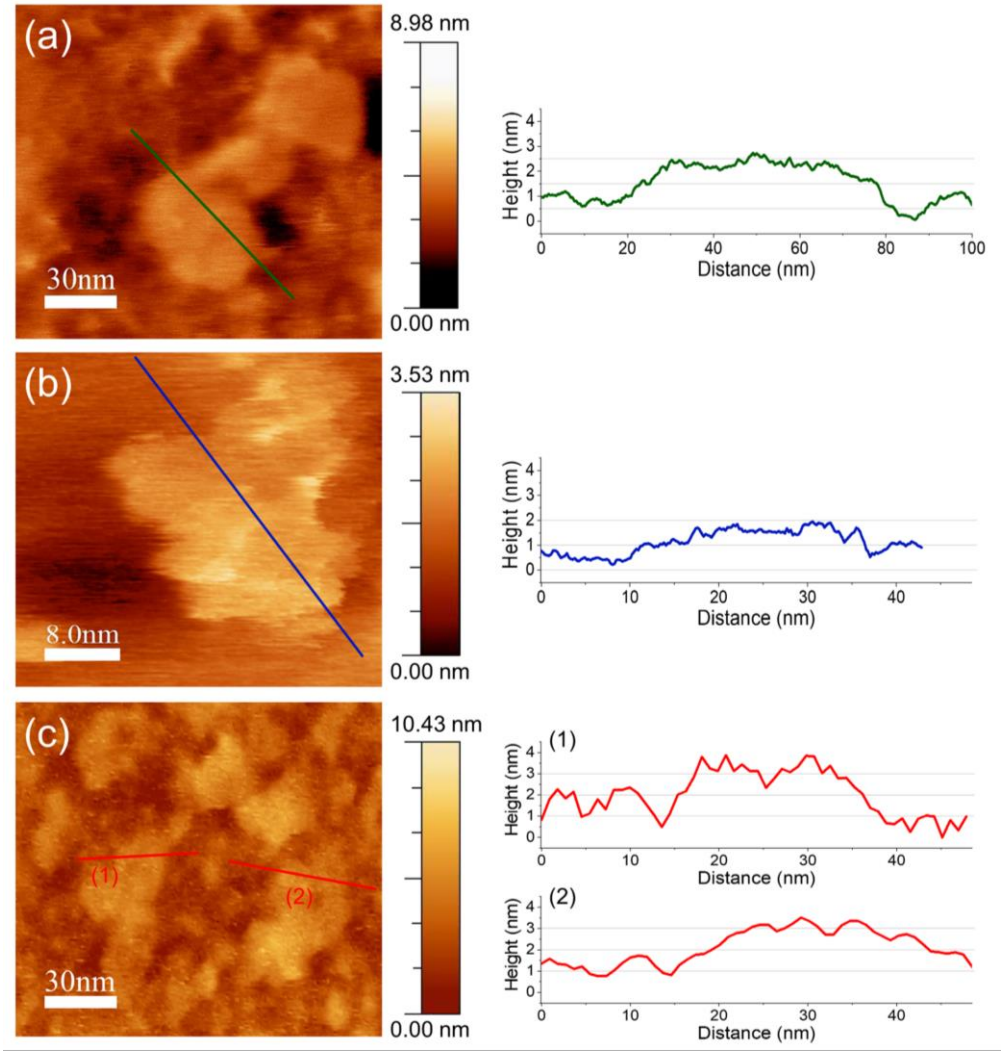

Figure S2. AFM height images of the nanosheets deposited on plasma-treated HOPG together with their corresponding height profiles. (a) AFM image of the HOPG/Ni LDH sheets in 0.1 M KOH. (b) AFM image of the HOPG/NiCo LDH sheets in 0.1 M KOH. (c) AFM image of the HOPG/NiFe LDH sheets at the air/solid interface.

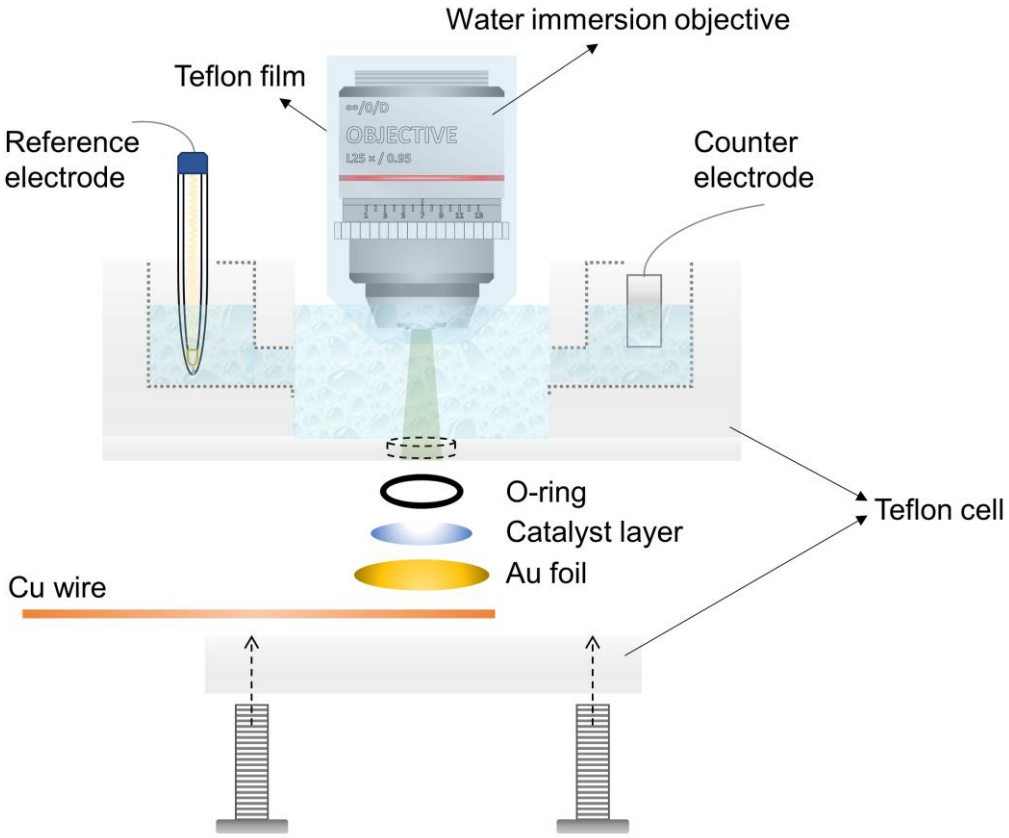

Figure S3. Experimental set-up for the *in-situ* Raman spectroscopy study.

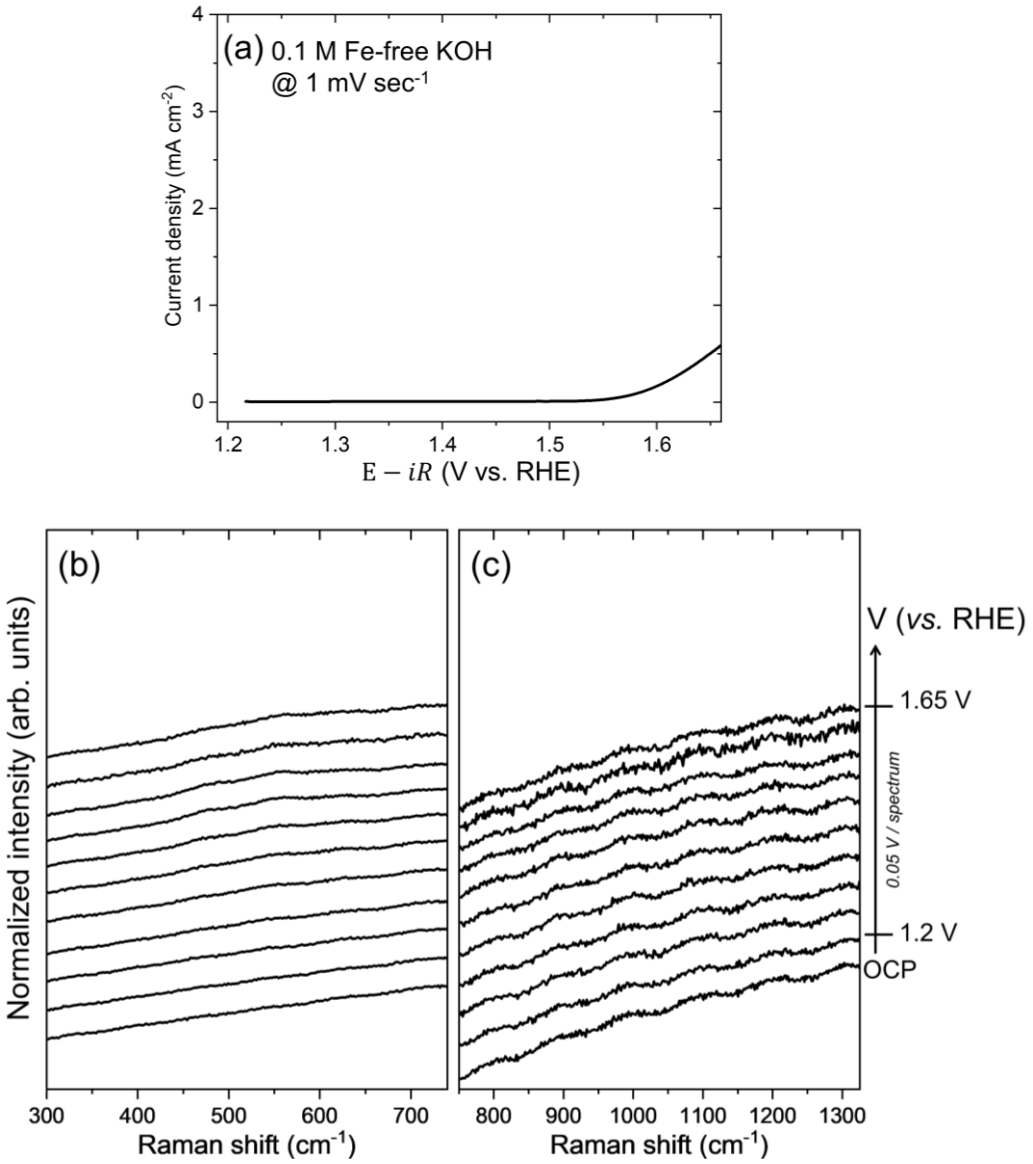

Figure S4. (a) LSVs of the Au substrate alone at the scan rate of 1 mV sec^{-1} in 0.1 M Fe-free KOH; *in-situ* Raman spectra obtained on the Au substrate alone in the regions where the peaks corresponding to (b) Ni-O and (c) $NiOO^{-}$ are normally observed at each constant potential from OCP to 1.65 V with the interval of 0.05 V.

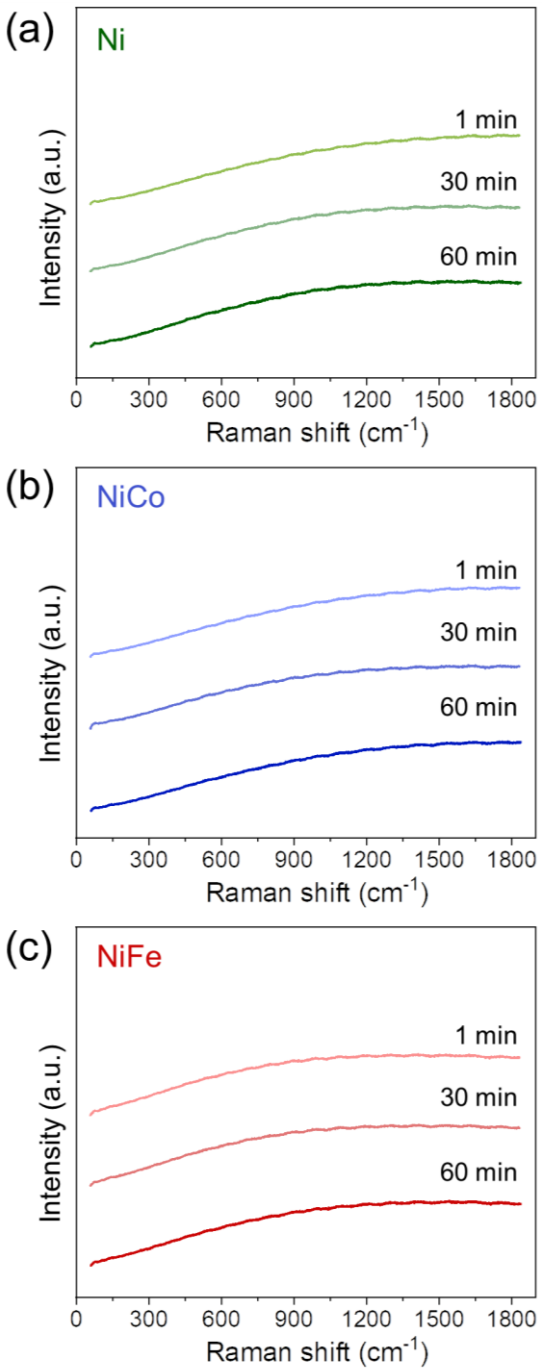

Figure S5. *In-situ* Raman spectra for Ni (a), NiCo (b) and NiFe LDH (c) at an open circuit potential (OCP). The data were obtained at the time interval of 1, 30, 60 min to examine whether the LDH surface changes by long-term exposure to the laser irradiation. The Raman peaks observed at OER potentials were absent at OCP even after a long-term exposure, suggesting no phase change due to laser irradiation.

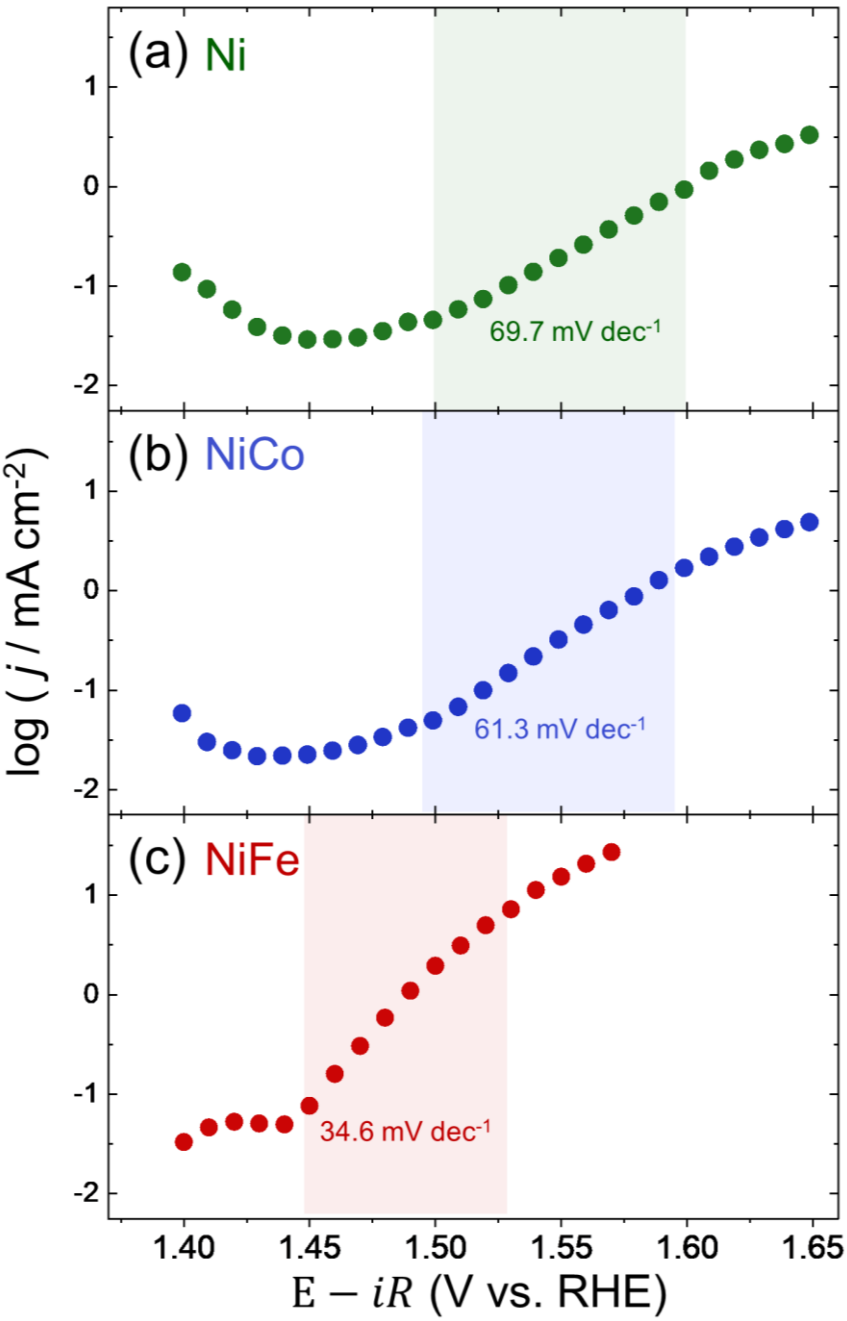

Figure S6. Comparison of Tafel slopes of (a) Ni, (b) NiCo and (c) NiFe LDH. Steady state currents at the end of 60 sec at each constant potential were chosen for the calculation of Tafel slope. The Tafel kinetic regime to obtain the Tafel slopes of each catalyst is highlighted in the figure.

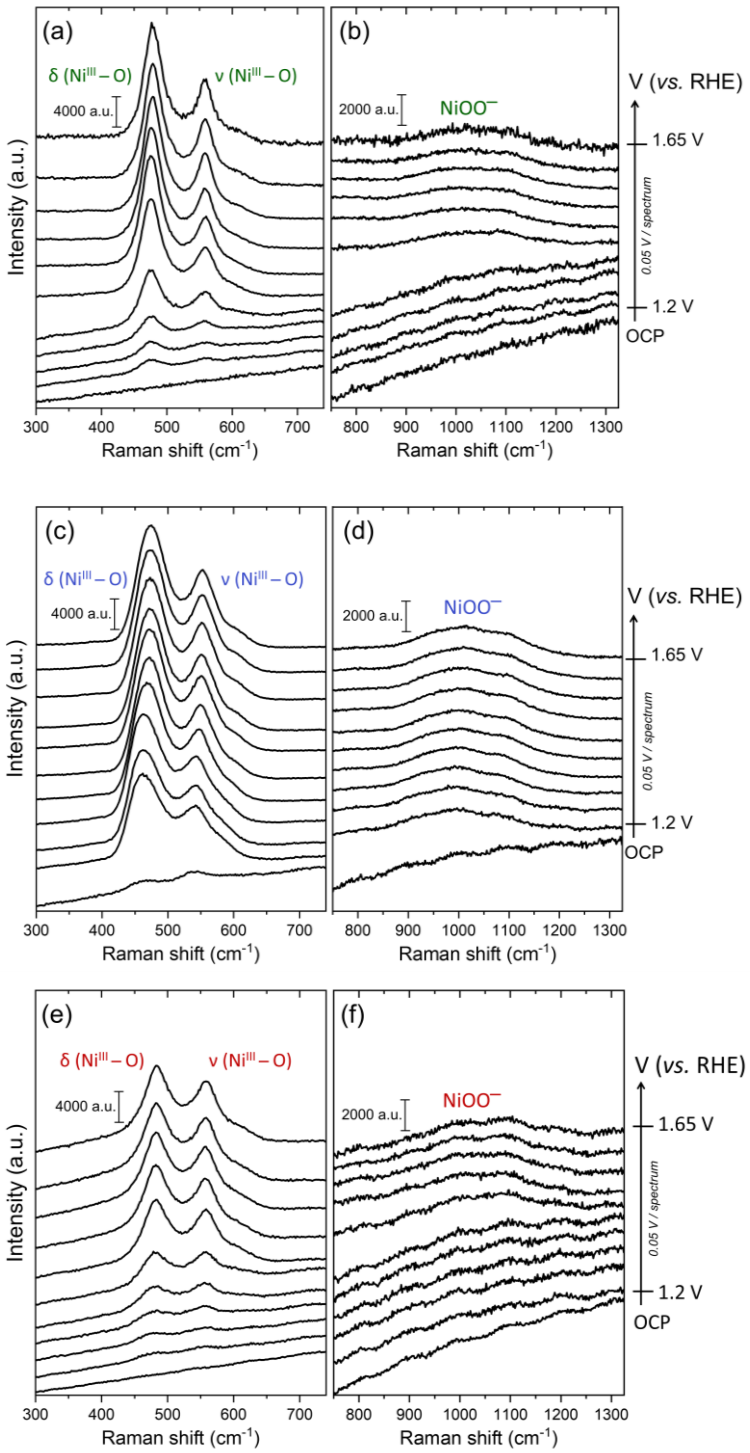

Figure S7. *In-situ* Raman spectra for Ni (a and b), NiCo (c and d) and NiFe LDH (e and f). The data were obtained at each constant potential in 0.1 M Fe-free KOH from OCP to 1.65 V and the interval was 0.05 V.

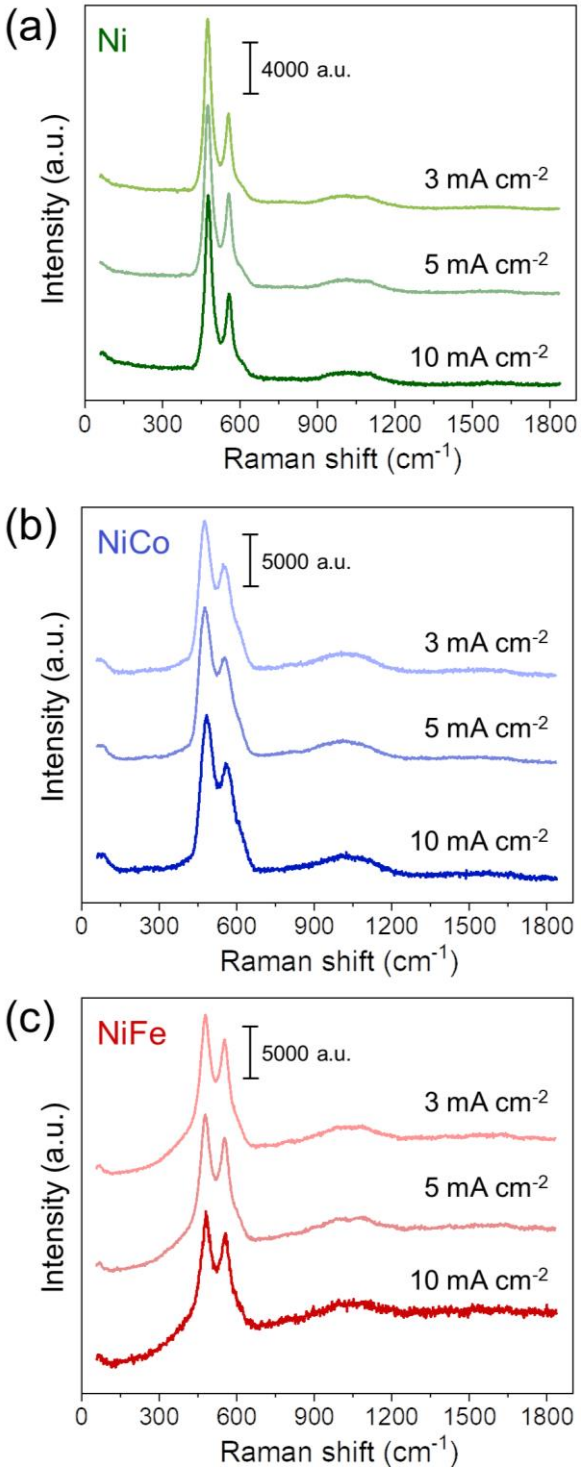

Figure S8. *In-situ* Raman spectra for Ni (a, NiCo (b) and NiFe LDH (c) collected under constant current densities in 0.1 M Fe-free KOH.

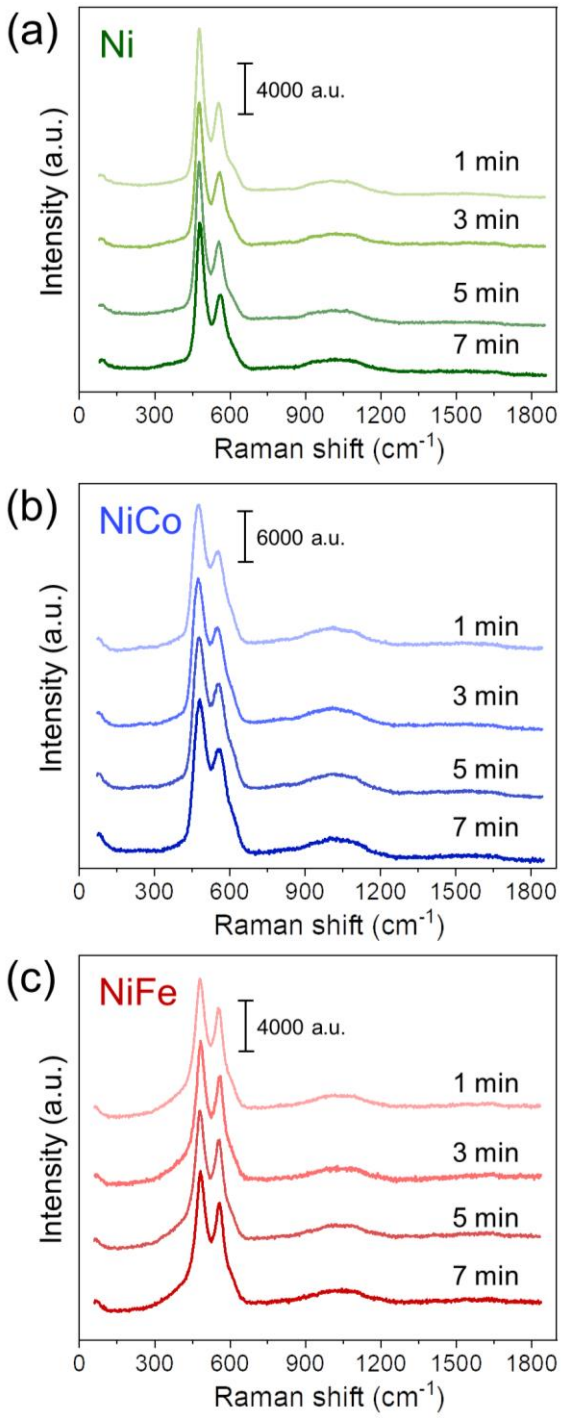

Figure S9. Raman spectra for Ni (a), NiCo (b) and NiFe LDH (c). The spectra were obtained at the open circuit potential after the samples were oxidized at 1.65 V for 3 min to reach $Ni^{III}MOOH$ (M = Co or Fe) phases.

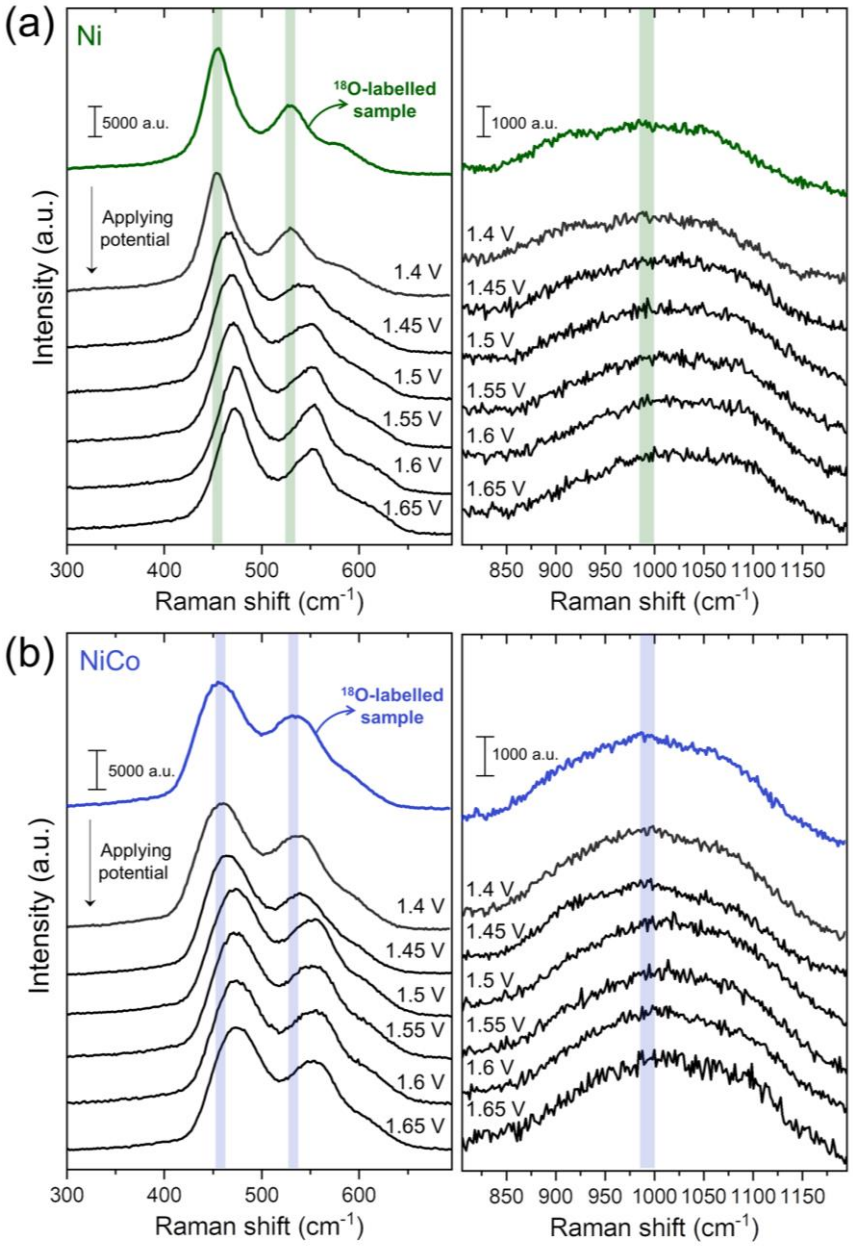

Figure S10. The isotope labelling experiment results for Ni and NiCo LDHs as a function of applied potentials.

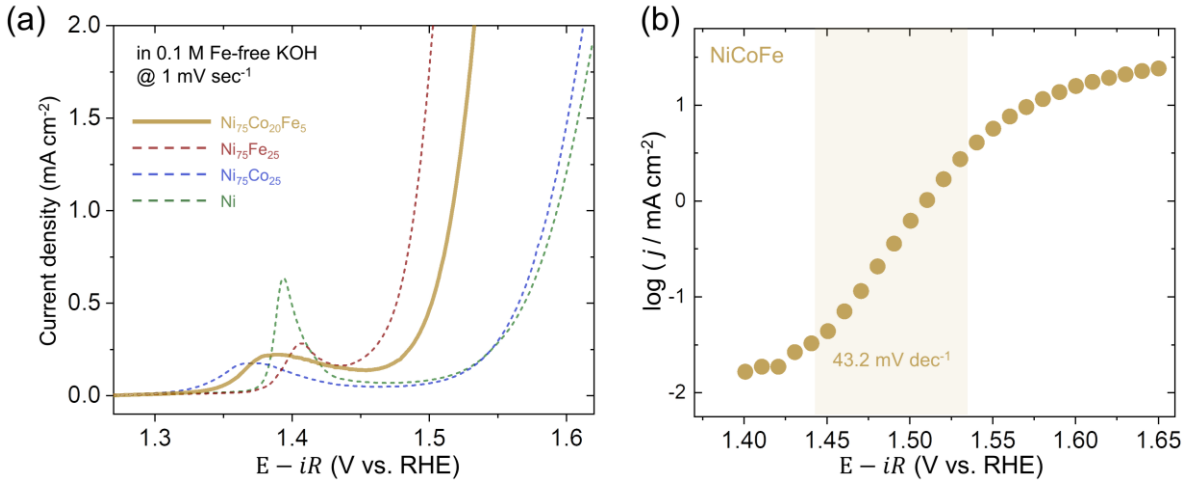

Figure S11. (a) LSV curves of NiCoFe (20% Co and 5% Fe) and comparison to those of other catalysts. (b) Tafel slope for NiCoFe LDH.

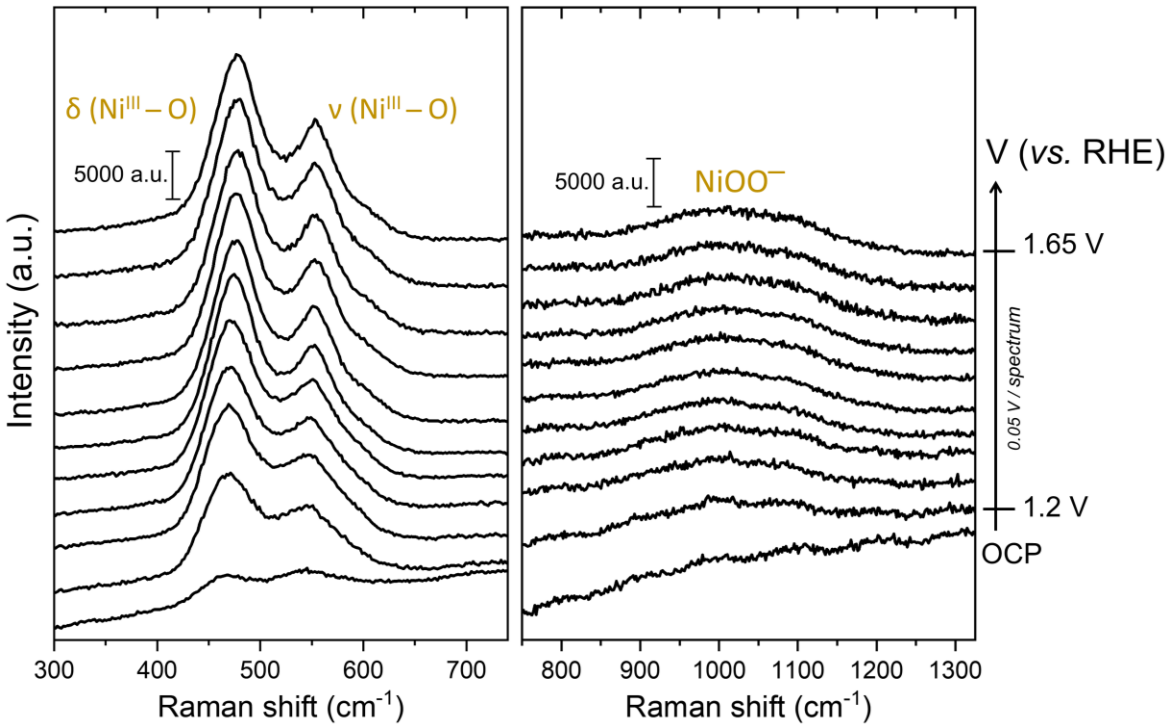

Figure S12. *In-situ* Raman spectra in the regions of Ni-O and NiO-O^{-} for NiCoFe LDH. The spectra were measured at each constant potential in 0.1 M Fe-free KOH from OCP to 1.65 V and the interval was 0.05 V.

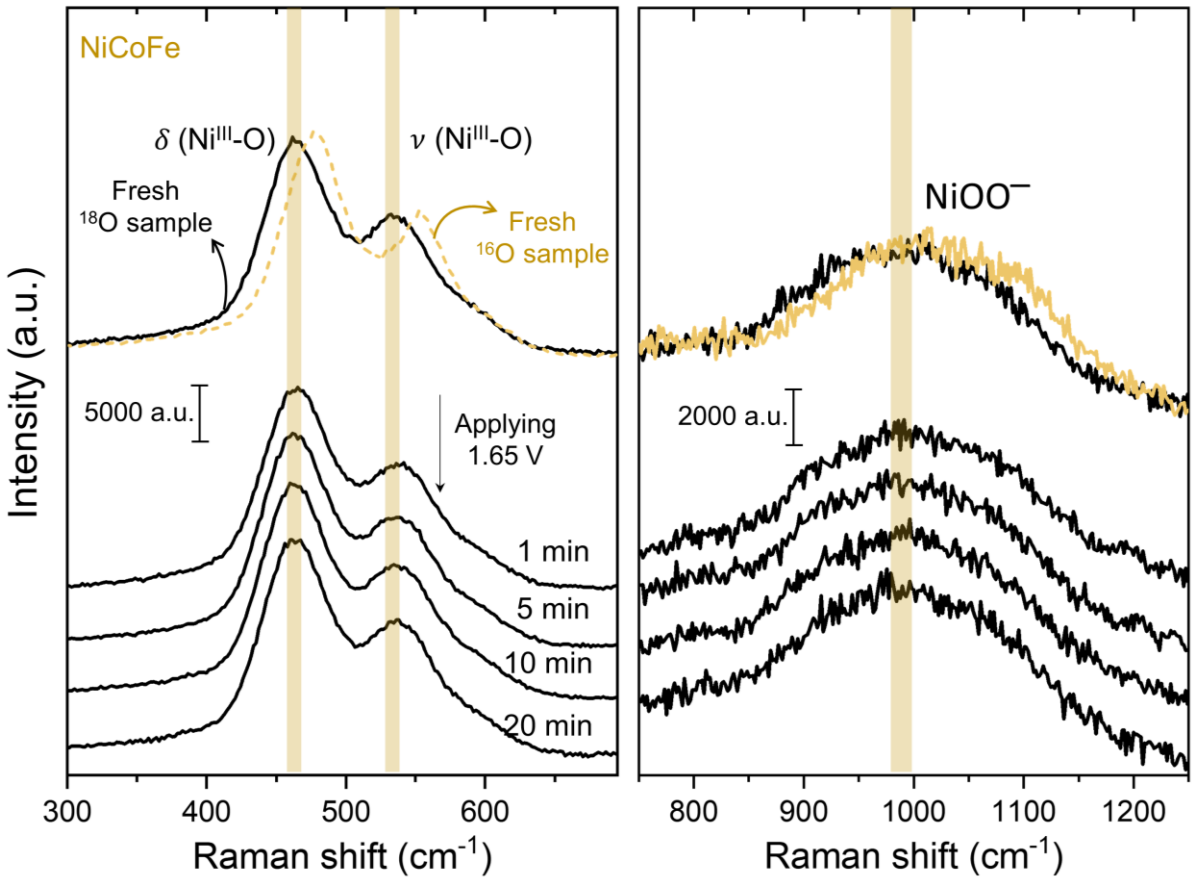

Figure S13. The isotope labelling experiment results for NiCoFe LDH.

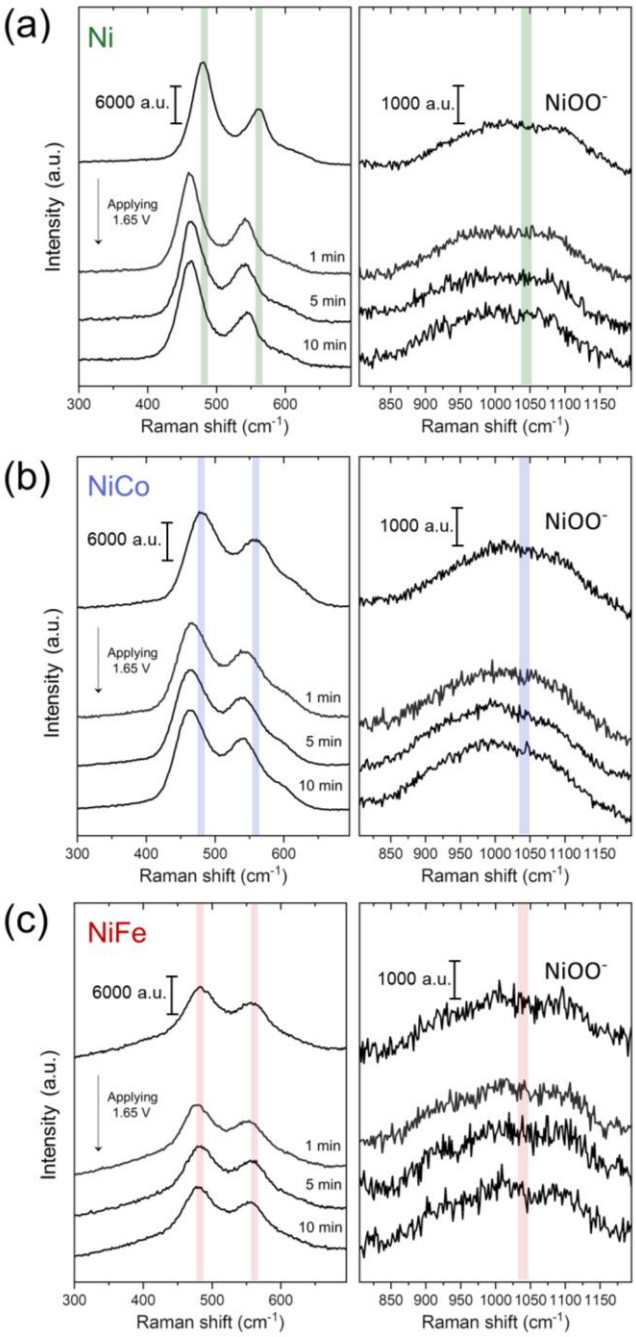

Figure S14. Isotope exchange experiments using oxidized forms of LDHs. The ^{16}O-labelled samples were first electrolyzed at 1.65 V in 0.1 M KOH for 3 min. Then *in-situ* Raman spectra were collected at 1.65 V in 0.1 M KOH of $H_2{}^{18}O$. Raman spectra of (a) Ni, (b) NiCo and (c) NiFe LDHs were shown. The Raman spectra were obtained in the regions of the Ni species such as NiOOH (left column) and $NiOO^-$ (right column). The peak shift due to the lattice oxygen exchange was observed for Ni and NiCo but the lattice oxygen of NiFe was not exchanged.

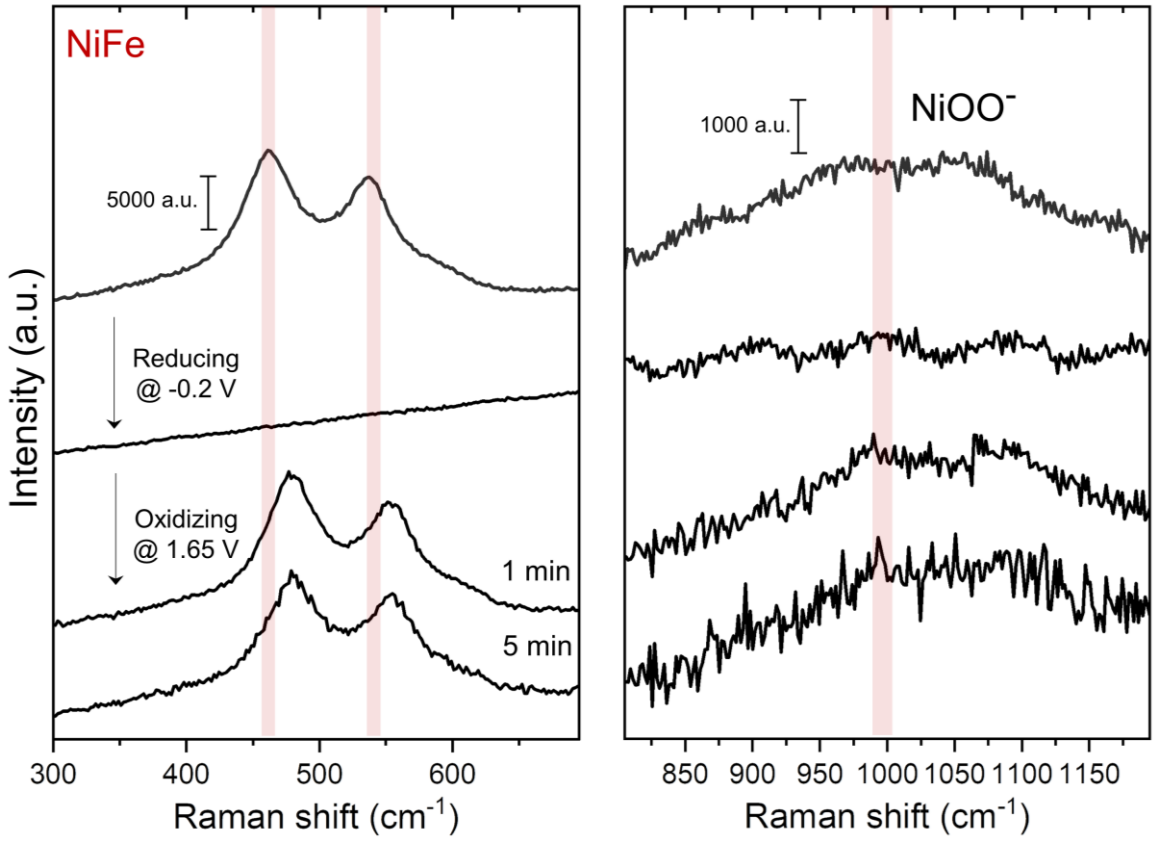

Figure S15. Raman spectra of ^{18}O-labelled NiFe LDH, where the sample was first oxidized to a Ni(III) form and then reduced to a Ni(II) form. The sample was then subject to electrolysis at 1.65 V in $^{16}OH_2$. The data show oxygen isotope exchange, in contrast to the experiments using oxidized NiFe LDH.

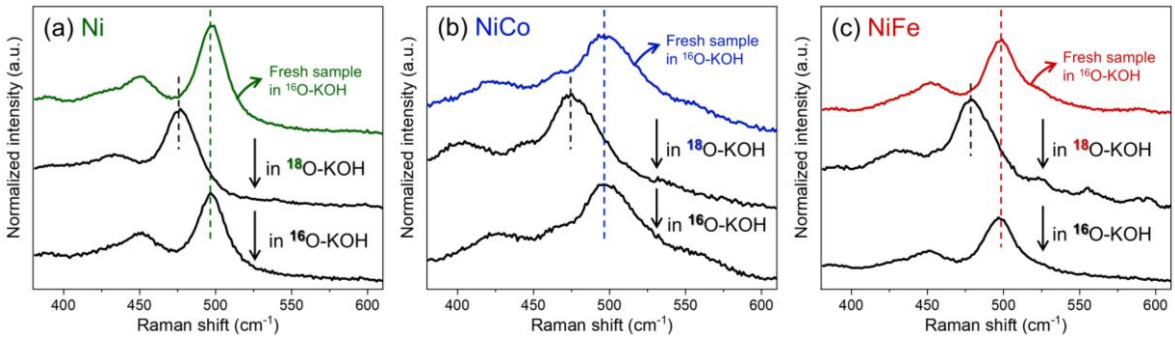

Figure S16. Raman spectra of the as-synthesized samples of (a) Ni, (b) NiCo and (c) NiFe LDHs obtained in ^{16}O-KOH and ^{18}O-KOH in the absence of applied potential. They were obtained at the laser wavelength of 785 nm to take advantage of the SERS effect for a high sensitivity. The Ni ions were in the oxidation state of +2.

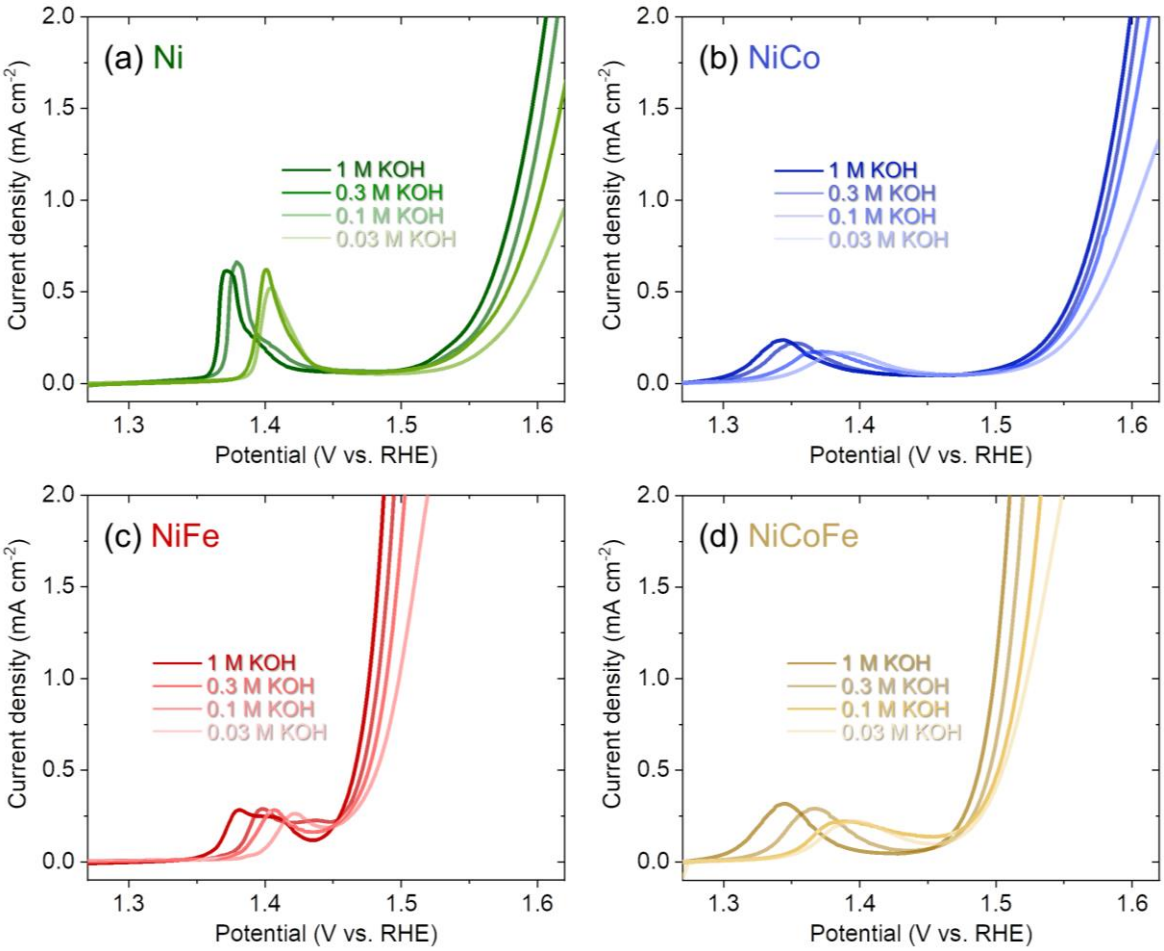

Figure S17. LSV curves of (a) Ni, (b) NiCo, (c) NiFe and (d) NiCoFe LDHs at different values of pH (*i.e.* 12.4 in 0.03 M KOH; 12.88 in 0.1 M KOH; 13.31 in 0.3 M KOH; 13.78 in 1 M KOH).

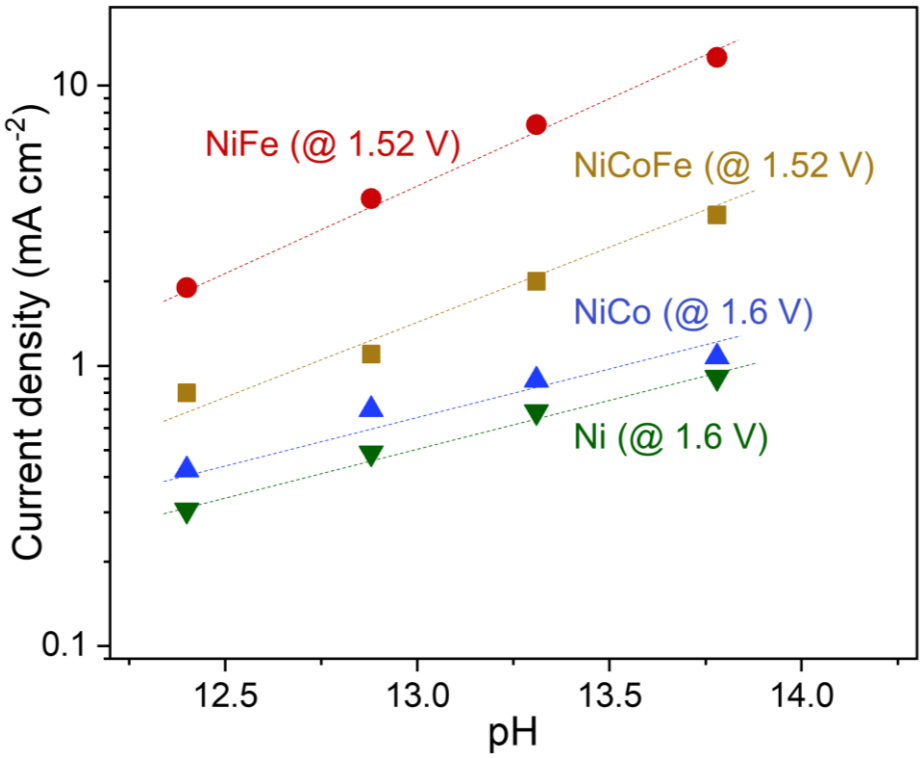

Figure S18. A plot for OER current density at 1.52 V for NiFe and NiCoFe and 1.6 V for Ni and NiCo as a function of pH. The potentials are referenced to RHE. The OER currents for all the samples increased with increasing pH values, which indicates pH-dependent OER activity at the RHE scale.[5]

References

[1] J. Yu, B. R. Martin, A. Clearfield, Z. Luo, L. Sun, *Nanoscale* **2015**, *7*, 9448-9451.

[2] I. Horcas, R. Fernández, J. Gomez-Rodriguez, J. Colchero, J. Gómez-Herrero, A. Baro, *Review of scientific instruments* **2007**, *78*, 013705.

[3] L. Trotochaud, S. L. Young, J. K. Ranney, S. W. Boettcher, *J Am Chem Soc* **2014**, *136*, 6744-6753.

[4] O. Diaz-Morales, D. Ferrus-Suspedra, M. T. M. Koper, *Chem Sci* **2016**, *7*, 2639-2645.

[5] A. Grimaud, O. Diaz-Morales, B. Han, W. T. Hong, Y. L. Lee, L. Giordano, K. A. Stoerzinger, M. T. M. Koper, Y. Shao-Horn, *Nat Chem* **2017**, *9*, 457-465.